J|A|C|S ARTICLES

Published on Web 07/29/2010

Ferro- and Antiferromagnetic Coupling Switch Accompanied by Twist Deformation around the Copper(II) and Nitroxide Coordination Bond

Atsushi Okazawa,[†,‡] Daisuke Hashizume,[§] and Takayuki Ishida*[,†]

Department of Applied Physics and Chemistry, The University of Electro-Communications, Chofu, Tokyo 182-8585, Japan, and Advanced Technology Support Division, RIKEN (Institute of Physical and Chemical Research), Wako, Saitama 351-0198, Japan

Received March 15, 2010; E-mail: ishi@pc.uec.ac.jp

Abstract: Two novel copper(II) complexes with *tert*-butyl 2-pyridyl nitroxide (2pyNO•), $[Cu^{2+}(2pyNO^{-})(2pyNO^{\bullet})]_2(BF_4^{-})_2$ (**1**·BF_4) and $[Cu^{2+}(2pyNO^{-})(2pyNO^{\bullet})]_2(ClO_4^{-})_2$ (**1**·ClO_4), were prepared and structurally characterized. They contained mixed-valent ligands from 2pyNO, whose oxygen atoms were located at equatorial positions of the copper ion. The $[Cu^{2+}(2pyNO^{-})(2pyNO^{\bullet})]$ unit was dimerized by μ-oxo bridges of the anion ligand, giving a zigzag linear spin system involving four paramagnetic $S = 1/2$ centers. The two compounds are isomorphous in an orthorhombic *Pbca* space group. Magnetic study revealed that **1**·ClO_4 showed ferromagnetic copper−radical coupling in all temperature ranges investigated here. On the other hand, **1**·BF_4 exhibited a structural phase transition at 64 K, where the magnetic susceptibility was drastically dropped on cooling. The copper−radical magnetic couplings were characterized as ferro- and antiferromagnetic for the high- and low-temperature phases, respectively. The crystallographic analysis clarified that the nitroxide oxygen atom remained at the equatorial position throughout the single-crystal-to-single-crystal phase transition, while the previously known spin-transition-like copper−radical compounds showed conversion of the roles of equatorial and axial positions. The orthogonal arrangement between the copper dσ and nitroxide π* orbitals is essential for the ferromagnetic coupling, and a slight dislocation of the radical oxygen atom from the chelate plane leads to violation of the orthogonal orbital arrangement, giving a practically diamagnetic low-temperature phase.

1. Introduction

Heterospin systems are attracting much attention from researchers in materials chemistry, because of the wide diversity of the characters of paramagnetic centers including the symmetry of the lobes of magnetic orbitals.[1−3] The mutual geometry of the magnetic orbitals has been controllable by choosing appropriate magnetic p, d, and/or f orbitals[4] and by applying synthetic techniques for metal−organic frameworks.[5] Orthogonal arrangement of magnetic orbitals such as combinations of e_g and t_{2g} d-orbitals and of π* and dσ orbitals has been well investigated,[6,7] which favors ferromagnetic coupling between the spins there.

Copper(II)−nitroxide coordination compounds are the best documented and characterized on the basis of their coordination geometry toward development of ferromagnetic materials.[8] A d^9 copper(II) ion has a well-defined magnetic orbital of $3d_{x^2-y^2}$, and a nitroxide group has an unpaired electron in the molecular

[†] UEC Tokyo.

[‡] Research Fellow of the Japan Society for the Promotion of Science. Present address: Department of Basic Science, Graduate School of Arts and Sciences, The University of Tokyo, Komaba, Meguro-ku, Tokyo 153-8902, Japan.

[§] RIKEN.

(1) Kahn, O. *Molecular Magnetism*; VCH Publishers: New York, 1993.

(2) *Molecular Magnetism: From Molecular Assemblies to the Devices*; Coronado, E., Delhaes, P., Gatteschi, D., Miller, J. S., Eds.; NATO Advanced Study Institute Series. Series E321, Applied Sciences; Kluwer Academic Publisher: Dordrecht, The Netherlands, 1996.

(3) (a) *Molecular Magnetism*; Itoh, K., Kinoshita, M., Eds.; Gordon and Breach Science Publisher: Amsterdam, The Netherlands, 2000. (b) *Molecular Magnets: Recent Highlights*; Linert, W., Verdaguer, M., Eds.; Springer-Verlag: Wien, Austria, 2003.

(4) (a) Sakamoto, M.; Hashimura, M.; Matsuki, K.; Matsumoto, N.; Inoue, K.; Okawa, H. *Bull. Chem. Soc. Jpn.* **1991**, *64*, 3639. (b) Kahn, M. L.; Mathoniere, C.; Kahn, O. *Inorg. Chem.* **1999**, *38*, 3692. (c) Bernot, K.; Bogani, L.; Caneschi, A.; Gatteschi, D.; Sessoli, R. *J. Am. Chem. Soc.* **2006**, *128*, 7947.

(5) (a) Yaghi, O. M.; Li, H.; Davis, C.; Richardson, D.; Groy, T. L. *Acc. Chem. Res.* **1998**, *31*, 474. (b) Eddaoudi, M.; Moler, D. B.; Li, H.; Chen, B.; Reineke, T. M.; O'Keeffe, M.; Yaghi, O. M. *Acc. Chem. Res.* **2001**, *34*, 319. (c) Stang, P. J.; Olenyuk, B. *Acc. Chem. Res.* **1007**, *30*, 502. (d) Kitagawa, S.; Kondo, M. *Bull. Chem. Soc. Jpn.* **1998**, *71*, 1739.

(6) (a) Okawa, H.; Nishida, Y.; Tanaka, M.; Kida, S. *Bull. Chem. Soc. Jpn.* **1977**, *50*, 127. (b) Kahn, O.; Galy, J.; Journaux, U.; Jaud, J.; Morgenstern-Badarau, I. *J. Am. Chem. Soc.* **1982**, *104*, 2165. (c) Tamaki, H.; Zhong, Z. J.; Matsumoto, N.; Kida, S.; Koikawa, M.; Achiwa, N.; Hashimoto, Y.; Okawa, H. *J. Am. Chem. Soc.* **1992**, *114*, 6974. (d) Mallah, T.; Thiebaut, S.; Verdaguer, M.; Veillet, P. *Science* **1993**, *262*, 1554. (e) Ferlay, S.; Mallah, T.; Ouahes, P.; Veillet, P.; Verdaguer, M. *Nature* **1995**, *378*, 701.

(7) (a) Bencini, A.; Benelli, C.; Gatteschi, D.; Zanchini, C. *J. Am. Chem. Soc.* **1984**, *106*, 5813. (b) Kahn, O.; Prins, R.; Reedijk, J.; Thompson, J. S. *Inorg. Chem.* **1987**, *26*, 3557.

(8) (a) Caneschi, A.; Gatteschi, D.; Sessoli, R.; Rey, P. *Acc. Chem. Res.* **1989**, *22*, 392. (b) Caneschi, A.; Gatteschi, D.; Rey, P. *Prog. Inorg. Chem.* **1991**, *39*, 331.

(9) (a) Dickman, M. H.; Doedens, R. J. *Inorg. Chem.* **1981**, *20*, 2677. (b) Porter, L. C.; Dickmann, M. H.; Doedens, R. J. *Inorg. Chem.* **1983**, *22*, 1962. (c) Porter, L. C.; Doedens, R. J. *Inorg. Chem.* **1985**, *24*, 1006. (d) Lim, Y. Y.; Drago, R. S. *Inorg. Chem.* **1972**, *11*, 1334.

 10.1021/ja102163d

π^* orbital. The magnetic coupling parameter J is typically determined as a singlet−triplet energy gap of $2J$ at a >NO−Cu unit. It has often been said that an equatorial binding results in a strong antiferromagnetic metal−radical exchange coupling ($J \ll 0$), while an axial coordination results in a moderate ferromagnetic coupling ($J > 0$).[8−10] However, Luneau and coworkers reported the considerable ferromagnetic couplings in the equatorially coordinated copper(II)−nitroxide systems,[11] and we have also studied and formulated the magneto−structure relationship in various ferro- and antiferromagnetic copper(II)− and nickel(II)−nitroxide compounds with respect to the orbital overlap between dσ and π^* magnetic orbitals.[12,13] Owing to the short distance and effective orbital interaction between the paramagnetic centers when coordinated equatorially, the magnetic couplings are considerably large whether ferromagnetic or antiferromagnetic.

There have been several reports on "spin-transition-like" copper(II)−nitroxide complexes,[10,14−20] in connection with spin-crossover transition metal complexes.[21,22] They involve a structural phase transition giving rise to a switch between local singlet and triplet states at the >NO−Cu unit, which is sometimes referred as two-centered spin-transition phenomena. Although the majority of molecule-based magnetic materials has been studied and analyzed with a constant J, we have to think of a temperature-dependent J in such compounds.[23] It has been suggested that the Cu−O bond lengths would change to convert the roles of axial and equatorial coordination sites,[10,14,17] which leads to switching ferro- and antiferromagnetic exchange interactions.

Chart 1. 2pyNO Radical and Anion

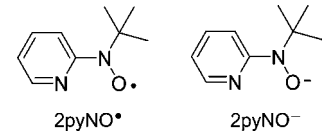

In the present paper, we will describe a new class of a spin-transition-like copper(II)−nitroxide complex by using a simple *tert*-butyl 2-pyridyl nitroxide (2pyNO•) as a paramagnetic chelating ligand (Chart 1),[12b,13] where the coordination site remains equatorial. The chemical composition does not change for the present compound, and such compounds seem to be of increasing interest for future applications to switching, sensing, and other devices.[21] Although the transition is drastic because the magnitude of the magnetic couplings is considerably large, the geometrical change is rather small to be monitored as a single-crystal-to-single-crystal phase transition. The mechanism of the spin-transition-like behavior can be unequivocally explained in terms of magneto−structure relationship. We will discuss the magneto-structure empirical equation using a simple geometrical parameter and comparison with the results on the metal−radical coordination compounds previously reported.

2. Results

2.1. Synthesis and Structural Characterization. We have previously prepared several copper(II)−nitroxide complexes, which contain a copper(II) ion and two 2-pyridyl substituted nitroxide radical ligands (L), $[Cu^{2+}(L)_2(X^-)_2]$ and $[Cu^{2+}(L)_2(H_2O)_2]^{2+}$ (X = ClO_4 or TfO; TfO = trifluoromethanesulfonate).[12b,13] On the

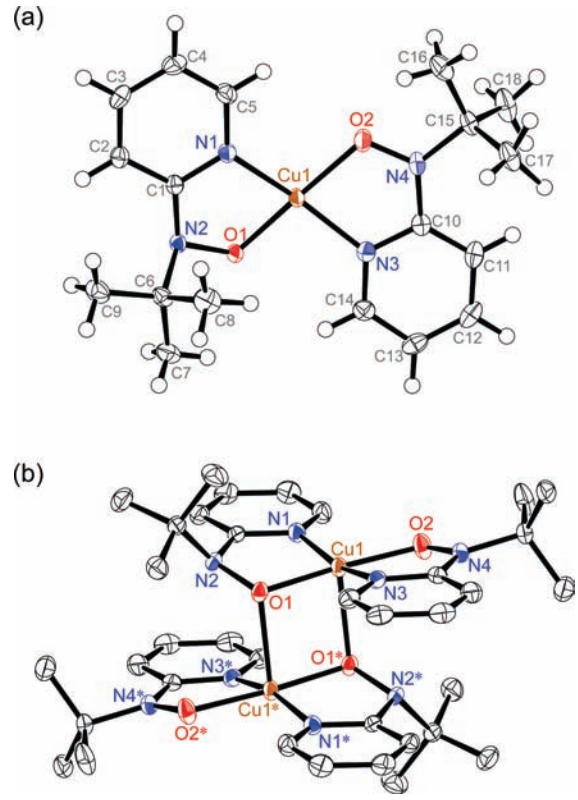

Figure 1. Molecular structures of (a) a mononuclear moiety $[Cu^{2+}(2pyNO^-)(2pyNO^•)]^+$ and (b) a dinuclear unit $[Cu^{2+}(2pyNO^-)(2pyNO^•)]_2^{2+}$ in **1**•ClO_4 with thermal ellipsoids at the 50% probability level. Atom numbering schemes are also shown. Hydrogen atoms are omitted in (b). The symmetry operation code of * is $-x$, $2-y$, $1-z$.

(10) de Panthou, F. L.; Belorizky, E.; Calemczuk, R.; Luneau, D.; Marcenat, C.; Ressouche, E.; Turek, P.; Rey, P. *J. Am. Chem. Soc.* **1995**, *117*, 11247.
(11) (a) Luneau, D.; Rey, P.; Laugier, J.; Fries, P.; Caneschi, A.; Gatteschi, D.; Sessoli, R. *J. Am. Chem. Soc.* **1991**, *113*, 1245. (b) Luneau, D.; Rey, P.; Laugier, J.; Belorizky, E.; Conge, A. *Inorg. Chem.* **1992**, *31*, 3578.
(12) (a) Osanai, K.; Okazawa, A.; Nogami, T.; Ishida, T. *J. Am. Chem. Soc.* **2006**, *128*, 14008. (b) Okazawa, A.; Nogami, T.; Ishida, T. *Chem. Mater.* **2007**, *19*, 2733.
(13) (a) Okazawa, A.; Nagaichi, Y.; Nogami, T.; Ishida, T. *Inorg. Chem.* **2008**, *47*, 8859. (b) Okazawa, A.; Nogami, T.; Ishida, T. *Polyhedron* **2009**, *28*, 1917.
(14) de Panthou, F. L.; Luneau, D.; Musin, R.; Ohrstrom, L.; Grand, A.; Turek, P.; Rey, P. *Inorg. Chem.* **1996**, *35*, 3484.
(15) Iwahori, F.; Inoue, K.; Iwamura, H. *Mol. Cryst. Liq. Cryst.* **1999**, *334*, 533.
(16) Caneschi, A.; Chiesi, P.; David, L.; Ferraro, F.; Gatteschi, D.; Sessoli, R. *Inorg. Chem.* **1993**, *32*, 1445.
(17) (a) Ovcharenko, V. I.; Fokin, S. V.; Romanenko, G. V.; Shvedenkov, Y. G.; Ikorskii, V. N.; Tretyakov, E. V.; Vasilevskii, S. F. *J. Struct. Chem.* **2002**, *43*, 153. (b) Ovcharenko, V. I.; Fokin, S. V.; Romanenko, G. V.; Ikorskii, V. N.; Tretyakov, E. V.; Vasilevskii, S. F.; Sagdeev, R. Z. *Mol. Phys.* **2002**, *100*, 1107. (c) Rey, P.; Ovcharenko, V. I. In *Magnetism: Molecules to Materials, IV*; Miller, J. S., Drillon, M., Eds.; Wiley-VCH: New York, 2003; pp 41−63.
(18) Maryunina, K.; Fokin, S.; Ovcharencko, V.; Romanenko, G.; Ikorskii, V. *Polyhedron* **2005**, *24*, 2094.
(19) Fedin, M.; Veber, S.; Gromov, I.; Maryunina, K.; Fokin, S.; Romanenko, G.; Sagdeev, R.; Ovcharenko, V.; Bagryanskaya, E. *Inorg. Chem.* **2007**, *46*, 11405.
(20) Hirel, C.; Li, L.; Brough, P.; Vostrikova, K.; Pecaut, J.; Mehdaoui, B.; Bernard, M.; Turek, P.; Rey, P. *Inorg. Chem.* **2007**, *46*, 7545.
(21) (a) *Spin Crossover in Transition Metal Compounds I, II, and III*; Gütlich, P., Goodwin, H. A., Eds.; Springer-Verlag: Berlin, 2004. (b) Gütlich, P.; Hauser, A.; Spiering, H. *Angew. Chem., Int. Ed. Engl.* **1994**, *33*, 2024.
(22) (a) Sato, O.; Tao, J.; Zhang, Z.-Z. *Angew. Chem., Int. Ed.* **2007**, *46*, 2152. (b) Sato, O.; Hayami, S.; Einaga, Y.; Gu, Z. Z. *Bull. Chem. Soc. Jpn.* **2003**, *76*, 443.
(23) Veber, S. L.; Fedin, M. V.; Potapov, A. I.; Maryunina, K. Y.; Romanenko, G. V.; Sagdeev, R. Z.; Ovcharenko, V. I.; Goldfarb, D.; Bagryanskaya, E. G. *J. Am. Chem. Soc.* **2008**, *130*, 2444.

Table 1. Selected Crystallographic Data for $\mathbf{1}_{HT}\cdot BF_4$, $\mathbf{1}_{LT}\cdot BF_4$, and $\mathbf{1}\cdot ClO_4$

compounds	$\mathbf{1}_{HT}\cdot BF_4$	$\mathbf{1}_{LT}\cdot BF_4$	$\mathbf{1}\cdot ClO_4$
formula	$C_{36}H_{52}B_2Cu_2F_8N_8O_4$	$C_{36}H_{52}B_2Cu_2F_8N_8O_4$	$C_{36}H_{52}Cl_2Cu_2N_8O_{12}$
formula weight	961.56	961.56	986.84
crystal system	orthorhombic	orthorhombic	orthorhombic
space group	*Pbca*	*Pbca*	*Pbca*
T/K	300	50	90
a/Å	20.012(1)	19.344(3)	19.771(15)
b/Å	17.270(1)	17.353(4)	17.178(15)
c/Å	12.711(1)	12.519(4)	12.672(11)
V/Å^3	4393.0(5)	4202.2(18)	4304(6)
Z	4	4	4
d_{calc}/g cm^{-3}	1.454	1.520	1.523
μ/mm^{-1}	1.049	0.761	1.181
λ/Å	0.71073	0.61792	0.71073
R_{int}	0.0569	0.0835	0.078
R (F)[a] ($I > 2\sigma(I)$)	0.0576	0.0415	0.0308
R_w (F^2)[b] (all data)	0.1726	0.1143	0.0388
G.O.F.	1.082	1.016	1.035
unique reflections	6013	23978	5339

[a] $R = \Sigma||F_o| - |F_c||/\Sigma|F_o|$. [b] $R_W = [\Sigma w(|F_o| - |F_c|)^2/\Sigma w|F_c|^2]^{1/2}$.

other hand, the complexes having diamagnetic 2pyNO$^-$ and 2pyNOH have also been developed.[24] To exploit mixed-valent compounds having both L$^\cdot$ and L$^-$, we tried complexation of 2pyNO$^\cdot$, 2pyNOH, and $CuX_2\cdot 6H_2O$ (X = BF_4 or ClO_4) with a rational molar ratio of 1/1/1 in a mixed dichloromethane−ethanol solvent, and actually we obtained $[Cu^{2+}(2pyNO^-)(2pyNO^\cdot)]_2(X^-)_2$ (abbreviated hereafter as $\mathbf{1}\cdot X$). The anionic 2pyNO$^-$ ligand was produced by deprotonation of 2pyNOH. The pyridyl moiety plays a role of a base.

The molecular structures $\mathbf{1}\cdot BF_4$ and $\mathbf{1}\cdot ClO_4$ were successfully determined by means of X-ray crystallographic analysis (Figure 1). Since $\mathbf{1}\cdot BF_4$ has two crystalline phases (see below), two X-ray diffraction data sets were collected as a high-temperature (HT) phase at 300 K and as a low-temperature (LT) phase at 50 K. Table 1 shows selected crystallographic data. The HT and LT phases of $\mathbf{1}\cdot BF_4$ ($\mathbf{1}_{HT}\cdot BF_4$ and $\mathbf{1}_{LT}\cdot BF_4$, respectively) and $\mathbf{1}\cdot ClO_4$ are isomorphous in the space group *Pbca* with the comparable cell parameters. Figure 1 shows the molecular structure of **1** in $\mathbf{1}\cdot ClO_4$, which are similar to those of $\mathbf{1}_{HT}\cdot BF_4$ and $\mathbf{1}_{LT}\cdot BF_4$. They form a centrosymmetric out-of-plane dimer (Figure 1b). The pyridine rings are arranged almost coplanar. Two counteranions per dimer unit were found in the clearance of the packing of the $[Cu^{2+}(2pyNO^-)(2pyNO^\cdot)]_2$ moiety (Figure 2). There are intradimer atomic contacts within the sum of the van der Waals radii[25] with respect to the pyridine rings (3.309(3) and 3.391(3) Å for the C1---C14* and C3---C13* distances, respectively).

Selected bond lengths and angles for each complex are listed in Table 2. The copper(II) ions were five-coordinated square-pyramidal, indicating the valence of Cu^{2+}. Two chelate rings are found, where two 2pyNO ligands are crystallographically independent. The axial position was occupied with the oxygen atom O1 of an adjacent anionic 2pyNO. The Cu−O1* distances (>2.3 Å) are somewhat long, compared with that of the equatorial bonds (1.9−2.0 Å), but the axial bonds are substantial because the O1 atom is dislocated from the basal plane toward Cu1*.

The inner oxygen atom (O1) bridges two Cu^{2+} ions but the outer one (O2) does not, suggesting the former is assigned to

(24) Okazawa, A.; Ishida, T. *Chem. Phys. Lett.* **2009**, *480*, 198.
(25) Bondi, A. *J. Phys. Chem.* **1964**, *68*, 441.

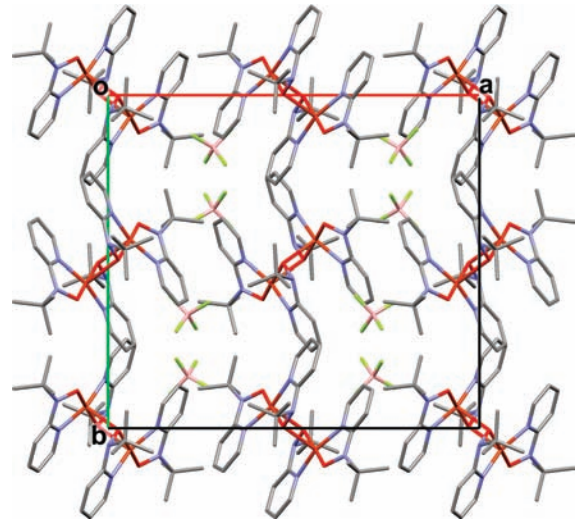

Figure 2. Molecular arrangement in the crystal of $\mathbf{1}_{LT}\cdot BF_4$ viewed along the *c* axis. Hydrogen atoms are omitted.

Table 2. Selected Interatomic Distances, Bond Angles, and Torsion Angles for $\mathbf{1}_{HT}\cdot BF_4$, $\mathbf{1}_{LT}\cdot BF_4$, and $\mathbf{1}\cdot ClO_4$

compounds	$\mathbf{1}_{HT}\cdot BF_4$	$\mathbf{1}_{LT}\cdot BF_4$	$\mathbf{1}\cdot ClO_4$
Cu1−O1	1.9040(19)	1.8963(6)	1.9081(13)
Cu1−N1	1.934(2)	1.9248(6)	1.9400(16)
Cu1−O2	1.977(2)	1.9819(7)	1.9837(15)
Cu1−N3	1.955(2)	1.9441(6)	1.9505(16)
Cu1−O1*	2.346(2)	2.3789(6)	2.3224(13)
Cu1−Cu1*	3.1629(5)	3.2276(5)	3.158(2)
O1−N2	1.417(3)	1.4092(8)	1.423(2)
O2−N4	1.298(3)	1.3025(8)	1.303(2)
Cu1−O1−Cu1*	95.63(8)	97.41(3)	96.08(5)
O1−Cu1−N1	82.21(9)	82.54(3)	82.08(6)
O1−Cu1−N3	98.65(9)	97.73(3)	98.22(6)
O2−Cu1−N1	99.99(9)	102.18(3)	100.33(6)
O2−Cu1−N3	80.17(10)	80.62(3)	80.21(6)
O1−N2−C1	110.87(19)	111.18(5)	110.92(13)
O1−N2−C6	109.1(2)	109.63(5)	109.49(14)
C1−N2−C6	119.6(2)	120.01(5)	119.64(16)
O2−N4−C10	116.6(2)	115.74(5)	116.79(16)
O2−N4−C15	115.5(3)	117.53(6)	116.44(16)
C10−N4−C15	127.8(2)	126.72(6)	126.73(16)
Cu1−O1−N2−C1	20.1(3)	17.65(7)	18.70(17)
Cu1−O2−N4−C10	4.5(3)	12.519(4)	2.1(2)
N1−Cu1−O1−N2	−16.74(17)	−15.08(4)	−15.81(11)
N3−Cu1−O2−N4	1.1(2)	−8.32(5)	2.59(12)

Chart 2. Selected Bond Lengths for $\mathbf{1}\cdot BF_4$. HT and LT Stand for the High- and Low-Temperature Phases, Respectively

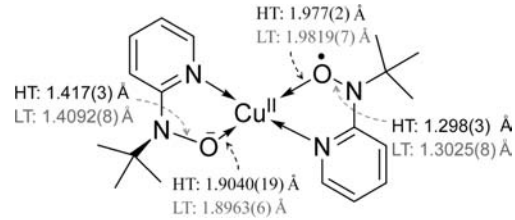

an anionic 2pyNO$^-$. This assignment is entirely consistent with detailed analysis of the geometry. The O1−N2 bond length of a inner 2pyNO ligand in $\mathbf{1}_{HT}\cdot BF_4$, was 1.417(3) Å (Chart 2), which is closer to the typical lengths for an aminoxide anion (1.45−1.47 Å for dimethylaminoxide[26]) and a hydroxylamine (1.456(4) Å for *N*-*tert*-butyl-*N*-phenylhydroxylamine[13a]) rather than those of the typical length for a nitroxide (1.28−1.32

Å).[13a,27] Furthermore, three angles around the nitrogen atom on the tertiary amine, O1−N2−C1, O1−N2−C6, and C1−N2−C6, were 113.2° on the average, indicating that this nitrogen atom has an sp^3-hybridized configuration (the ideal angle is 109.5°), expected for 2pyNO$^-$ and 2pyNOH.[24,26,27] Furthermore, the Cu1−O1 distance (1.9040(19) Å) was shortened compared with typical copper(II)−radical equatorial bond lengths (1.93−2.03 Å[12,13]). These findings imply that the inner ligand is anionic. In contrast, the O2−N4 bond length on the outer ligand was 1.298(3) Å, being the typical length for a nitroxide. Three angles around the nitrogen atom on the tertiary amine, O2−N4−C10, O2−N4−C15, and C10−N4−C15, were 120.0° on the average. It indicates that this nitrogen atom has an sp^2-hybridization (the ideal angle is 120°).[12,13,27] In addition, the Cu1−O2 distance is 1.977(2) Å, which is a typical length for a copper(II)−nitroxide equatorial coordinate bond.[12,13] Therefore, the outer ligand is paramagnetic.

According to the conventional Robin-Day classification of mixed-valence complexes,[28] the compound belongs to the Class I (localized)[29] as for the ligands. A similar analysis clarified that $\mathbf{1}_{LT}\cdot BF_4$ and $\mathbf{1}\cdot ClO_4$ had an anion and a radical ligand per a mononuclear unit. Therefore, the whole molecule has four localized $S = 1/2$ spins, which form a zigzag linear spin-system along the radical−copper−copper−radical array.

The interdimer copper−copper, copper−nitroxide, and nitoxide−nitroxide distances were longer than 7.8 Å. No meaningful interdimer interaction, such as a $\pi-\pi$ stacking or an interaction through counteranion, was observed in the crystal structures. Thus, the interdimer magnetic interaction is negligible for magnetic analysis.

We have proposed that the torsion angle ϕ along M−O−N−C_{2py} is a convenient indicator for the orthogonality.[13] The Cu1−O2−N4−C10 torsion angles $|\phi|$ are 4.5(3)°, 12.519(4)°, and 2.1(2)° for $\mathbf{1}_{HT}\cdot BF_4$, $\mathbf{1}_{LT}\cdot BF_4$, and $\mathbf{1}\cdot ClO_4$, respectively. Note that the two phases of $\mathbf{1}\cdot BF_4$ showed considerably different values of the torsion despite the practically identical crystal structure.

2.2. Magnetic Properties. Magnetic susceptibilities of $\mathbf{1}\cdot BF_4$ and $\mathbf{1}\cdot ClO_4$ were measured on a SQUID magnetometer (Figure 3). The $\chi_{mol}T$ value for a dinuclear unit of $\mathbf{1}\cdot BF_4$ was 1.463 cm^3 K mol^{-1} at 300 K, which is smaller than the calculated spin-only value (1.50 cm^3 K mol^{-1}) for the sum of the paramagnetic contributions of two copper(II) ions and two nitroxide radicals. An antiferromagnetic interaction is present in the dimer. Upon cooling from 300 to 68 K, the $\chi_{mol}T$ value of $\mathbf{1}\cdot BF_4$ slightly decreased (1.151 cm^3 K mol^{-1} at 68 K). On further cooling, the $\chi_{mol}T$ value abruptly approached zero below 68 K. This finding indicates that spin-transition-like behavior occurred around 68 K, after which the metal-radical coupling drastically changed to very strongly antiferromagnetic (see below).

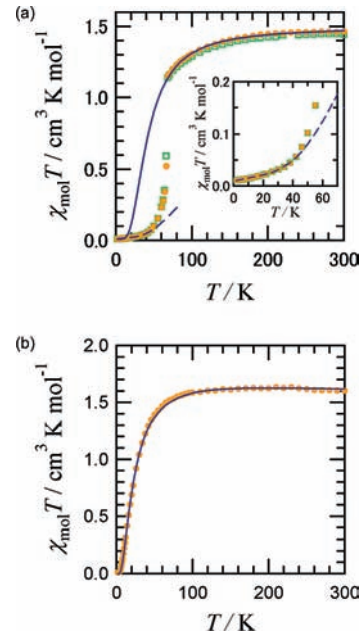

Figure 3. Temperature dependences of $\chi_{mol}T$ for polycrystalline samples of (a) $\mathbf{1}\cdot BF_4$ and (b) $\mathbf{1}\cdot ClO_4$ on the dimer basis. The applied magnetic fields were 5000 Oe. The orange filled circles and green open squares represent experimental data upon heating and cooling, respectively. The solid line in (a) is the theoretical best fit on the data in 80−300 K with $g_{avg} = 2.001(5)$, $J/k_B = +37(8)$ K, $j/k_B = -40(2)$ K. Inset shows a magnification of the plot. The dashed line is the best fit on the data in 1.8−34 K with $g_{avg} = 2.05$ (fixed), $J/k_B = -389(6)$ K, $j/k_B = -40$ K (fixed), $p = 0.942(1)$, and $\chi_{TIP} = 599(16) \times 10^{-6}$ cm^3 mol^{-1}. The solid line in (b) was the theoretical best fit on the data in 1.8−300 K with $g_{avg} = 2.035(2)$ K, $J/k_B = +109(2)$ K, and $j/k_B = -36.2(4)$ K. See the text for details on the equations.

The $\chi_{mol}T$ vs T plot of $\mathbf{1}\cdot ClO_4$ was significantly different from those of $\mathbf{1}\cdot BF_4$. The $\chi_{mol}T$ value was almost constant (1.60−1.63 cm^3 K mol^{-1}) from 300 to 120 K. This value is slightly larger than the calculated spin-only value. Obviously, the ferromagnetic interaction takes place between the metal-radical or metal−metal spin centers. On cooling, the $\chi_{mol}T$ values below 100 K decreased and approached almost zero around 1.8 K. However, no sudden drop of the $\chi_{mol}T$ value was observed. The intermolecular magnetic interaction was negligible because of no appreciable intermolecular interaction in the crystal packing. The null $\chi_{mol}T$ value indicates that the molecule has a ground singlet state.

The variable-temperature X-band electron-paramagnetic-resonance (EPR) measurements (Figures S1 and S2 in Supporting Information) were qualitatively consistent with the SQUID results. The spectra on $\mathbf{1}_{HT}\cdot BF_4$ and $\mathbf{1}\cdot ClO_4$ were similar to each other. The broad peaks were observed, and accordingly it was difficult to estimate precisely the g values. The broad peak of $\mathbf{1}_{LT}\cdot BF_4$ was weakened on cooling from ca. 60 K, and disappeared except for an impurity signal due to an isolated copper(II) ion. On the other hand, the broad peak of $\mathbf{1}\cdot ClO_4$ remained below 50 K. Therefore, the diamagnetic spin state of $\mathbf{1}_{LT}\cdot BF_4$ was confirmed, which appeared below the structural phase-transition temperature, while $\mathbf{1}\cdot ClO_4$ did not undergo any phase or spin transition.

We tried fitting the magnetic susceptibilities to estimate intramolecular magnetic interactions. There are four $S = 1/2$ centers in a molecule, and as Scheme 1 shows, we assumed the

(26) (a) Wang, R.; Zhang, X.-H.; Chen, S.-J.; Yu, X.; Wang, C.-S.; Beach, D. B.; Wu, Y.-D.; Xue, Z.-L. *J. Am. Chem. Soc.* **2005**, *127*, 5204. (b) Chen, S.-J.; Zhang, X.-H.; Yu, X.; Qui, H.; Yap, G. P. A.; Guzei, I. A.; Lin, Z.; Wu, Y.-D.; Xue, Z.-L. *J. Am. Chem. Soc.* **2007**, *129*, 14408. (c) Venugopal, A.; Berger, R. J. F.; Willner, A.; Pape, T.; Mitzel, N. W. *Inorg. Chem.* **2008**, *47*, 4506.
(27) (a) Kurokawa, G.; Ishida, T.; Nogami, T. *Chem. Phys. Lett.* **2004**, *392*, 74. (b) Nishimaki, H.; Mashiyama, S.; Yasui, M.; Nogami, T.; Ishdia, T. *Chem. Mater.* **2006**, *18*, 3602. (c) Inoue, K.; Iwamura, H. *Adv. Mater.* **1992**, *4*, 801. (d) Fujita, J.; Tanaka, M.; Suemune, H.; Koga, N.; Matsuda, K.; Iwamura, H. *J. Am. Chem. Soc.* **1996**, *118*, 9347. (e) Fujita, J.; Matsuoka, Y.; Matsuo, K.; Tanaka, M.; Akita, T.; Koga, N.; Iwamura, H. *Chem. Commun.* **1997**, 2393.
(28) Robin, M. B.; Day, P. *Adv. Inorg. Chem. Radiochem.* **1967**, *10*, 247.
(29) Lu, C. C.; Bill, E.; Weyhermüller, T.; Bothe, E.; Wieghardt, K. *J. Am. Chem. Soc.* **2008**, *130*, 3181.

Scheme 1. Exchange Coupling Model of the Dinuclear Core in $\mathbf{1}^{2+}$

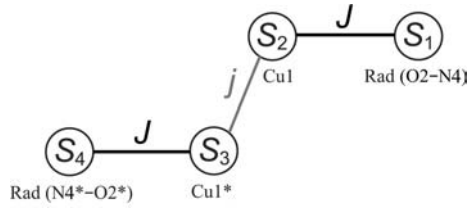

couplings in adjacent spin centers were appreciable; the copper-radical interaction J at the direct chelation and the superexchange Cu−O···Cu interaction j. The >NO−Cu coupling is unique due to the inversion symmetry in the dimeric structure. The Heisenberg spin-Hamiltonian was defined as $H = -2J(S_1 \cdot S_2 + S_3 \cdot S_4) - 2jS_2 \cdot S_3$, and we applied the Heisenberg, Dirac, and van Vleck equation[30] to the present system. We obtained:[31]

$$\chi_{\mathrm{mol}} = \frac{N_{\mathrm{A}} g_{\mathrm{avg}}^2 \mu_{\mathrm{B}}^2}{k_{\mathrm{B}} T} \frac{A}{B} \tag{1}$$

where

$$A = 10 \exp(-E_1/k_{\mathrm{B}}T) + 2 \exp(-E_2/k_{\mathrm{B}}T) + 2 \exp(-E_3/k_{\mathrm{B}}T) + 2 \exp(-E_4/k_{\mathrm{B}}T)$$

$$B = 5 \exp(-E_1/k_{\mathrm{B}}T) + 3 \exp(-E_2/k_{\mathrm{B}}T) + 3 \exp(-E_3/k_{\mathrm{B}}T) + 3 \exp(-E_4/k_{\mathrm{B}}T) + \exp(-E_5/k_{\mathrm{B}}T) + \exp(-E_6/k_{\mathrm{B}}T)$$

$$E_1 = -J - j/2,\ E_2 = J - j/2$$

$$E_3 = j/2 + \sqrt{J^2 + j^2},\ E_4 = j/2 - \sqrt{J^2 + j^2}$$

$$E_5 = J + j/2 + \sqrt{4J^2 - 2Jj + j^2}$$

and

$$E_6 = J + j/2 - \sqrt{4J^2 - 2Jj + j^2}$$

We can apply all of the data on $\mathbf{1}_{\mathrm{HT}}\cdot BF_4$, $\mathbf{1}_{\mathrm{LT}}\cdot BF_4$, and $\mathbf{1}\cdot ClO_4$, to eq 1, because they are isomorphous. Actually we used the data of $\mathbf{1}_{\mathrm{HT}}\cdot BF_4$ in the range 80−300 K, giving the following optimized parameters: $J/k_{\mathrm{B}} = +37(8)$ K, $j/k_{\mathrm{B}} = -40(2)$ K, and $g_{\mathrm{avg}} = 2.001(5)$. The intramolecular metal-radical coupling is ferromagnetic. An introduction of the temperature-independent paramagnetism term (χ_{TIP}) caused a lower reliability in the fit, and the χ_{TIP} value was small. This term was approximately neglected in the analysis. The optimized g value apparently is unrealistic from the reported g_{avg} values of copper(II)−radical of typically 2.05.[12,13] In this analysis an additional parameter p was introduced as a purity factor in eq 1. A possible impurity is paramagnetic $[Cu^{2+}(2pyNO^-)_2]$, and the Curie impurity term is reasonably assumed with $C_{\mathrm{imp}} = 0.402$ cm^3 K mol^{-1} (i.e., $g = 2.07$)[32] in eq 2. The parameters were optimized as $p = 0.947(6)$, $J/k_{\mathrm{B}} = +37(8)$ K, and $j/k_{\mathrm{B}} = -40(2)$ K with g_{avg} value fixed to be 2.05. Note that the magnetic exchange parameters would never be changed regardless of the introduction of p, and therefore the exchange parameter values are quantitatively reliable in any analysis.

$$\chi_{\mathrm{mol}} = p \frac{N_{\mathrm{A}} g_{\mathrm{avg}}^2 \mu_{\mathrm{B}}^2}{k_{\mathrm{B}} T} \frac{A}{B} + (1 - p) \frac{C_{\mathrm{imp}}}{T} \tag{2}$$

The ferromagnetic copper−nitroxide coupling in $\mathbf{1}_{\mathrm{HT}}\cdot BF_4$ is compatible with the finding that the chelate ring around the metal−radical moiety has a small torsion (Cu−O−N−C_{2py} = 4.5(3)° at 300 K). However, from a close look at quantitative analysis, the magnitude of J in the present compound is smaller than that of calculation from the torsion angle ϕ.[13]

The exchange parameters in $\mathbf{1}_{\mathrm{LT}}\cdot BF_4$ can be analyzed on the same model. The data in a temperature range below 34 K, which corresponds to the pure LT phase region as clarified by the XRD study (see below), were applied to eq 2. However, the J and j values could not be satisfactorily refined, probably owing to an overparametrization for a poor temperature dependence of $\chi_{\mathrm{mol}}T$. As an approximation, j is fixed to the value of the HT phase (−40(2) K), because the geometry around Cu1−O1−Cu1* is not so much deformed across the transition temperature (for example, the Cu1−O1−Cu1* angles are 95.63(8) and 97.41(3)° for the HT and LT phases, respectively). The g_{avg} and C_{imp} parameters were also fixed to be 2.05 and 0.402 cm^3 K mol^{-1}, respectively, for the same reason.

Fitting to the resultant expression afforded optimized parameters: $p = 0.942(1)$, $J/k_{\mathrm{B}} = -389(6)$ K, and $\chi_{\mathrm{TIP}} = 599(16) \times 10^{-6}$ cm^3 mol^{-1}. The largely negative J with the large $|\phi|$ is consistent with the magneto−structure relationship. A χ_{TIP} term was added here, and the value was much larger than a typical value (about 60×10^{-6} cm^3 mol^{-1} per Cu^{2+} ion).[1] A possible critical behavior (incomplete transition for example) just below the phase transition temperature would lead to an increase of $\chi_{\mathrm{mol}}T$ and give rise to an apparent overestimation of χ_{TIP} in this numerical fitting.

The Cu···Cu superexchange interaction j across the μ-oxide bridge was antiferromagnetic. The correlations between the singlet−triplet energy gap $2j$ and several geometrical parameters have been investigated for various [CuX_2Cu]-type dimers having a parallel-planar (out-of-plane) geometry.[33−35] Although several out-of-plane copper dimers have been reported to show ferromagnetic coupling,[33,36] antiferromagnetic couplings were also reported on the structures similar to the present one (the Cu−X···Cu angles of 98.5(1), 97.9(1), and 96.1(1)°).[37] It seems to be natural that the magneto−structural correlation would depend on the types of bridging-groups. To the best of our

(30) (a) Heisenberg, W. Z. *Physik* **1926**, *38*, 411. (b) Dirac, P. A. *Proc. R. Soc. London* **1926**, *112A*, 661. (c) van Vleck, J. H. *The Theory of Electric and Magnetic Susceptibilities*; Oxford University Press: Oxford, UK, 1932.
(31) Hall, J. W.; Estes, W. E.; Estes, E. D.; Scaringe, R. P.; Hatfield, W. E. *Inorg. Chem.* **1977**, *16*, 1572.
(32) This compound was prepared in 47% yield from an ethanol solution containing 2pyNOH, 1,8-diazabicyclo[5.4.0]undec-7-ene, and $Cu(ClO_4)_2\cdot 6H_2O$. Elemental analysis, spectroscopic analysis, and X-ray crystallographic analysis satisfied the formula of $[Cu(2pyNO)_2]$. Magnetic measurements indicated that the Curie constant was 0.4022(4) cm^3 K mol^{-1} with a negligible Weiss temperature.
(33) (a) Roundhill, S. G. N.; Roundhill, D. M.; Bloomquist, D. R.; Landee, C.; Willett, R. D.; Dooley, D. M.; Gray, H. B. *Inorg. Chem.* **1979**, *18*, 831. (b) Marsh, W. E.; Patel, K. C.; Hatfield, W. E.; Hodgson, D. J. *Inorg. Chem.* **1983**, *22*, 511.
(34) Hatfield, W. E.; Weller, R. R.; Hall, J. W. *Inorg. Chem.* **1980**, *19*, 3825.
(35) (a) Chiari, B.; Helms, J. H.; Piovesana, O.; Tarantelli, T.; Zanazzi, P. F. *Inorg. Chem.* **1986**, *25*, 2408. (b) Escrivà, E.; Sever-Carrió, J.; Lezama, L.; Folgado, J.-V.; Pizarro, J. L.; Ballesteros, R.; Abarca, B. *J. Chem. Soc., Dalton Trans.* **1997**, 2003.
(36) Zang, Y.; Yin, Z.; Wang, G.; Zeng, C.; Dai, A.; Zhou, Z. *Inorg. Chem.* **1990**, *29*, 560.

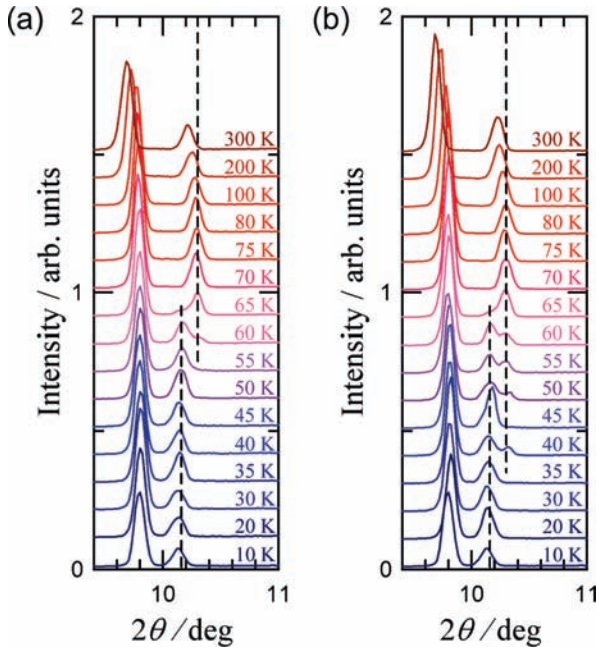

Figure 4. Powder XRD patterns of **1**·BF_4 upon (a) heating and (b) cooling at given temperatures. Dotted lines lie at $2\theta = 10.15°$ and 10.3°.

knowledge, the present aminoxide bridge is a quite rare example compared with the hydroxide and alkoxide bridges.

Compound **1**·ClO_4 has a unique phase, and accordingly the magnetic parameters were simply analyzed on the basis of eq 1 in an entire temperature range. The parameters were successfully optimized to give $J/k_B = +109(2)$ K, $j/k_B = -36.2(4)$ K, and $g_{avg} = 2.035(2)$. The torsion angle around Cu−O−N−C_{2py} for **1**·ClO_4 is smaller than that for $\mathbf{1}_{HT}$·BF_4. As we expected, the J value of **1**·ClO_4 is larger than that of $\mathbf{1}_{HT}$·BF_4. The j value was estimated to be moderately antiferromagnetic, as in the case of **1**·BF_4. In the [CuX_2Cu] out-of-plane dimers with the same μ-bridging group, there seems to be a correlation between the intramolecular interaction j and structural parameters around the [CuX_2Cu] core.[33−35] The present result is acceptable because the Cu1−O1−Cu1* geometries were similar to each other ($\mathbf{1}_{HT}$·BF_4: 95.63(8)°, **1**·ClO_4: 96.08(5)°).

2.3. Structural Phase Transition. To obtain evidence of the structural phase transition of **1**·BF_4 at ~68 K, the powder X-ray diffraction (XRD) analysis was performed on varying temperature. The XRD patterns for **1**·BF_4 were recorded at several temperatures in the range 10−300 K ($8° < 2\theta < 30°$). Figure 4 shows the temperature dependences of the 1 1 1 and 0 2 0 reflections on heating and cooling processes. The 0 2 0 reflections around $2\theta = 10.2°$ were divided into two signals between 60 and 65 K, and then the peaking angle was shifted to a lower direction on lowering temperature. This discontinuity implies a first-order phase transition.

It seems quite unusual that the b axis was lengthened on cooling across the phase transition temperature (T_C). Figure 5 shows the temperature dependence of the relative cell constant and unit cell volume from 10 K with respect to the room-temperature values. On cooling across T_C, the b length became longer, while the a length shortened, and the cell volume V shrank. The 0 2 0 reflections of LT and HT phases were both present in 60−65 K on heating. Similarly, both of them were found in 65−40 K on cooling. This finding is incompatible with the absence of thermal hysteresis in the magnetic study. It is probably because of a pinning effect of the structural phase

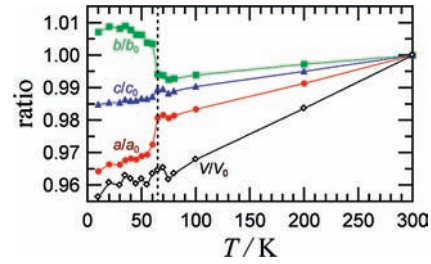

Figure 5. Temperature dependence of the relative cell constants for **1**·BF_4 with respect to the values at room temperature (300 K). Solid line is drawn for a guide to the eye. Dotted line indicates the structural phase transition around 65 K.

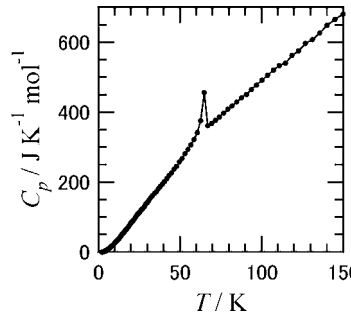

Figure 6. Heat capacity of **1**·BF_4 at zero field measured on cooling. Solid line is drawn for a guide to the eye.

transition from the crystal defects present in a finely ground powder form specifically prepared for the XRD study.

To examine the phase transition independently, we studied the heat capacity on **1**·BF_4. The temperature dependence of the molar specific heat C_p for **1**·BF_4 is displayed in Figure 6. The zero-field specific heat shows an anomaly around 64 K, which corresponds to the phase transition detected by the magnetic susceptibility and the XRD measurements. The T_C was determined to be 64 K by the peak of C_p. The heating and cooling runs afforded the same transition temperature, in agreement with the results of the magnetic study. The phase transition entropy was preliminarily estimated to be >7.6 J K^{-1} mol^{-1}. This value suggests that the phase transition involves not only the spin transition but also the transition enthalpy change,[38] i.e., this phase transition is a first-order one. The extrapolated normal heat capacity of the two phases usually exhibits a gap ΔC_p for several spin-crossover systems.[38] In the present study, a slight larger heat capacity was found in the high-temperature phase, but the quantitative analysis should not be made because of the limitation of the accuracy in the relaxation technique.

2.4. A Proposed Mechanism. Spin-transition-like copper(II)−radical compounds have been found in several *tert*-butyl nitroxide and nitronyl nitroxide complexes.[10,14−20] These materials have the mutual conversion of the axial−equatorial roles during a structural phase transition, and thus the magnetic interactions between copper ions and radicals are changed.[10,14,17] However, the Cu1−O2 coordination bond length in **1**·BF_4 was practically unchanged (from 1.977(2) to 1.9844(17) Å), but the

(37) (a) Manzur, J.; Mora, H.; Vega, A.; Spodine, E.; Venegas-Yazigi, D.; Garland, M. T.; Fallah, M. S. E.; Escuer, A. *Inorg. Chem.* **2007**, *46*, 6924. (b) Che, D.-J.; Li, G.; Yao, X.-L.; Zhu, Y.; Zhou, D.-P. *J. Chem. Soc., Dalton Trans.* **1999**, 2683. (c) Chiari, B.; Helms, J. H.; Piovesana, P.; Tarantelli, T.; Zanazzi, P. F. *Inorg. Chem.* **1986**, *25*, 2408.
(38) (a) Sorai, M.; Burriel, R.; Westrum, E. F., Jr.; Hendrickson, D. N. *J. Phys. Chem. B* **2008**, *112*, 4344. (b) Sorai, M.; Seki, S. *J. Phys. Soc. Jpn.* **1972**, *33*, 575.

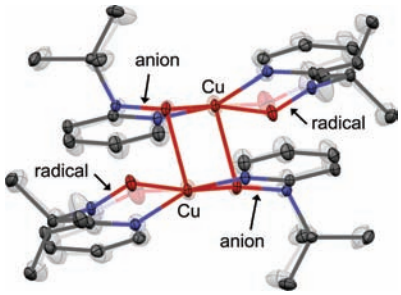

Figure 7. Superimposed molecular structures of the HT (300 K) and LT phases (50 K) of $\mathbf{1}\cdot BF_4$, shown by shaded and solid drawings, respectively. Note that the dislocation of the 2pyNO• oxygen atom from the chelate plane is appreciable in LT phase.

Cu1−O2−N4−C10 torsion was drastically changed (from 4.5(3) to 12.519(4)) across the phase transition. The axial−equatorial-conversion mechanism does not hold for $\mathbf{1}\cdot BF_4$. Furthermore, the valences of 2pyNO ligands were maintained, and thus the possibility of any electron transfer between a 2pyNO ligand and a copper(II) ion should be eliminated.

Ovcharenko and co-workers recently reported tough crystals of nitroxide−copper(II) compounds during polymorphous transformation.[39,40] Significant structural rearrangements in the complex usually give rise to breakdown of the crystals,[10,14,15] and phase transitions without such breakdown occur rarely. One of typical examples exploited by them is the polymeric $Cu(hfac)_2$ and *N*-methylpyrazolyl nitronyl nitroxide,[39] which showed the shortening of the Cu−O(radical) distance by 0.49 Å and elongation of the Cu−O(hfac) distance by 0.32 Å on cooling across the phase transition temperature; namely, the radical oxygen atom displaces into an equatorial position. As a consequence, the weak ferromagnetic interaction at the high-temperature phase changes to the strong antiferromagnetic interaction at the low-temperature phase. In some cases,[39] the weak antiferromagnetic interaction at the high-temperature phase changes to the moderate antiferromagnetic interaction in the low-temperature phase. In comparison with their results, $\mathbf{1}\cdot BF_4$ exhibited much milder structural transformation and much more drastic switching behavior due to the change from the ferromagnetic coupling to the strong antiferromagnetic coupling. Note that the nitroxide oxygen atom of $\mathbf{1}\cdot BF_4$ remained at the equatorial position throughout the transition.

Figure 7 shows the very subtle atomic motion between $\mathbf{1}_{HT}\cdot BF_4$ and $\mathbf{1}_{LT}\cdot BF_4$. The picture clearly indicates that there was no remarkable motion around $[CuO_2Cu]$ core or the anion ligands. Instead, a small structural deformation on 2pyNO ligands was observed. Although the torsion angle around Cu1−O2−N4−C10 appreciably changed, the *tert*-butyl group virtually does not move. The change of the torsion angle around the coordination bonds is a direct trigger to the magnetic coupling switch. The present compound can be regarded as a new class of spin-transition systems.

No phase transition was found for $\mathbf{1}\cdot ClO_4$. We have to mention the structural difference between $\mathbf{1}\cdot ClO_4$ and $\mathbf{1}\cdot BF_4$. The BF_4 anions are located in a clearance among pyridine rings and *tert*-butyl groups. Three C−H···F contacts were found in $\mathbf{1}_{HT}\cdot BF_4$, which are located approximately parallel to the *bc* plane. There is no other significant intermolecular contact within the sum of the van der Waals radii. It indicates that the molecular packing is relatively loose along the *a* axis, which may facilitate molecular motion in the solid phase. On the other hand, after the phase transition, the number of the C−H···F contacts in $\mathbf{1}_{LT}\cdot BF_4$ increased from three sites to nine due to the lattice shrinkage in a three-dimensional manner.

The cell volumes in the crystal of $\mathbf{1}_{HT}\cdot BF_4$ and $\mathbf{1}\cdot ClO_4$ at 90 K are 4229 $Å^3$ (estimated from Figure 5) and 4304(6) $Å^3$, respectively. The difference in ionic size between BF_4^- and ClO_4^- ions is small (ionic radius $r(BF_4^-) = 2.84$ Å, $r(ClO_4^-) = 2.90$ Å),[41] and accordingly the volume difference from the eight counteranions is expected to be only 50 $Å^3$. On the other hand, the difference of the cell volumes actually is 75 $Å^3$. It also implies that the molecular packing of $\mathbf{1}\cdot BF_4$ was tighter than that of $\mathbf{1}\cdot ClO_4$. Therefore, we assume that the chance whether the solid−solid phase transition occurs is related with the steric congestion of the molecules in the solid phase. The peripheral 2pyNO radicals, which are more flexible to move than the inner 2pyNO anions, were distorted by the chemical pressure from the BF_4^- anion on cooling. Intermolecular repulsive interaction may be a driving force of the intramolecular deformation.

2.5. Magneto−Structure Relationship. Now we check the magneto−structure relationship previously described on metal−radical compounds,[13] where a nitroxide radical (*tert*-butyl nitroxide or nitronyl nitroxide) chelated at an equatorial position of a first-transition metal ion carrying dσ spins (copper(II) and nickel(II) ions). The range of the magnetic coupling is notably wide and very sensitive to the change of the chelate structure.[42] The geometrical torsion parameter ϕ around the metal−radical bond has been proposed to be a simple and convenient indicator.[13]

We have previously drawn a plot of J versus ϕ for the hexacoordinated nickel(II) and copper(II) complexes and now have superimposed the points obtained from the present compounds on the same plot (Figure 8). The present results are largely downward deviated from the previous plot. It is simply ascribable to the difference of the magnetic orbitals between the present five-coordinated and the previous six-coordinated complexes. The metal center is dislocated above the basal plane in a square pyramidal geometry, and accordingly, the magnetic oribital $3d_{x^2-y^2}$ may not be defined to be located strictly on the *xy* plane. A smaller J is rationalized by partial cancellation with a considerable orbital overlap between the nitroxide π^* and copper(II) $3d_{x^2-y^2}$ orbitals. Furthermore, the antiferromagnetic coupling is more sensitive to ϕ in the present compounds than those in the square planar compounds.

The magneto−structure relationship for $\mathbf{1}\cdot BF_4$ and $\mathbf{1}\cdot ClO_4$ is formulated as $2J/k_B = a + b|\phi|$ with $a = 337(13)$ K and $b = -57.8(3)$ K deg^{-1}. The critical $|\phi|$, at which the sign of the metal−radical exchange coupling changes from positive to negative, is 5.83(4)°. The coupling is very sensitive to ϕ. The magnitude is considerably large whether it is ferromagnetic or antiferromagnetic. This result supports that the present exchange coupling model basically holds for various equatorially chelated

(39) Ovcharenko, V. I.; Maryunina, K. Y.; Fokin, S. V.; Tretyakov, E. V.; Romanenko, G. V.; Ikorskii, V. N. *Russ. Chem. Bull. Int. Ed.* **2004**, *53*, 2406.
(40) (a) Fokin, S.; Ovcharenko, V. I.; Romanenko, G.; Ikorskii, V. *Inorg. Chem.* **2004**, *43*, 969. (b) Ovcharenko, V. I.; Romanenko, G. V.; Maryunina, K. Y.; Bogomyakov, A. S.; Gorelik, E. V. *Inorg. Chem.* **2008**, *47*, 9537. (c) Veber, S. L.; Fedin, M. V.; Maryunina, K. Y.; Romanenko, G. V.; Sagdeev, R. Z.; Baryanskaya, E. G.; Ovcharenko, V. I. *Inorg. Chim. Acta* **2008**, *361*, 4148.
(41) (a) Weast, R. C., Ed. *Handbook of Chemistry and Physics*; CRC Press: Boca Raton, FL, 1987. (b) Nakamura, H.; Sunatsuki, Y.; Kojima, M.; Matsumoto, N. *Inorg. Chem.* **2007**, *46*, 8170.
(42) Ovcharenko, V. I.; Romanenko, G. V.; Ikorskii, V. N.; Musin, R. N.; Sagdeev, R. Z. *Inorg. Chem.* **1994**, *33*, 3370.

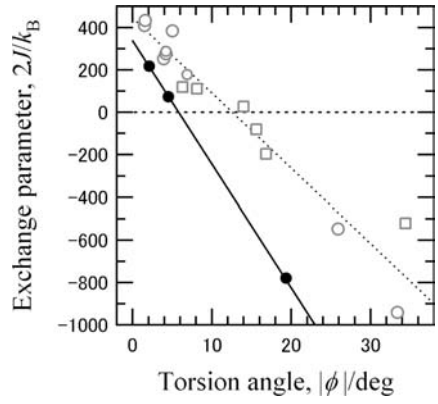

Figure 8. Plot of the observed exchange coupling parameter ($2J$) versus M−O−N−C_{2Ar} torsion angle ($|\phi|$) as a magneto−structure relationship in the six-coordinated nickel(II) or copper(II) complexes with radical chelating ligands. Filled circles stand for the data points on $\mathbf{1}_{HT}\cdot BF_4$, $\mathbf{1}_{LT}\cdot BF_4$, and $\mathbf{1}\cdot ClO_4$ (five-coordinated copper(II) ions). The data of aryl *tert*-butyl nitroxide compounds (open circles) and aryl nitronyl nitroxide complexes (open squares) were taken from ref 13 and the references cited therein. The dashed and solid lines stand for linear fits for six-coordinated and five-coordinated copper(II) complexes, respectively.

metal−radical systems, with an optimization of the parameters a and b in the common phenomenological formula $2J/k_B = a + b|\phi|$.

A model compound (Figure 9) for estimating the exchange coupling parameter between copper−radical was simplified by replacing the 2pyNO anion group with a 2pyNOH group and *tert*-butyl groups with methyl ones, and density functional theory (DFT) calculations were performed at the UB3LYP/6-311G(d,p) level[43,44] on the Gaussian03 program.[45] The parameter J's were +236, −764, and +352 K for $\mathbf{1}_{HT}\cdot BF_4$, $\mathbf{1}_{LT}\cdot BF_4$, and $\mathbf{1}\cdot ClO_4$, respectively, from the calculated singlet−triplet energy gap (Table 3). We confirmed that the small $|\phi|$ value would cause the large J value, despite somewhat overestimation for $\mathbf{1}_{HT}\cdot BF_4$ and $\mathbf{1}\cdot ClO_4$. The calculation study revealed that a relatively small geometrical change would cause a considerably large change in magnetic properties in the present system.

3. Summary

We prepared two mixed-ligand copper(II) complexes $\mathbf{1}\cdot BF_4$ and $\mathbf{1}\cdot ClO_4$, and structurally characterized them by X-ray crystallographic analysis. They are practically isomorphous, but only $\mathbf{1}\cdot BF_4$ underwent a structural phase transition at $T_c = 64$ K. The phase transition was confirmed from the studies of XRD and heat capacity, together with magnetic susceptibility on $\mathbf{1}\cdot BF_4$. Intramolecular copper−radical coupling was changed from ferromagnetic to antiferromagnetic on cooling, accompanied by a single-crystal-to-single-crystal phase transition. The crystallographic analysis revealed the following plausible mechanism. A small Cu−O−N−C_{2py} torsion favors ferromagnetic coupling due to the intrinsic orthogonality between the magnetic do−π* orbitals in the equatorial coordination. A geometrical torsion leads to antiferromagnetic coupling in a very sensitive manner, and the equatorial coordination of the nitroxide group is retained across the structural phase transition. A novel mechanism has been thus clearly demonstrated.

Magnetic coupling switch in $\mathbf{1}\cdot BF_4$ is drastic. We are investigating a material having the new spin-transition-like behavior, which obeys the magneto−structure relationship for six-coordinated complexes. Such a material may drastically change the magnetic interactions from strongly ferromagnetic to strongly antiferromagnetic with the energy comparable with that of a room temperature, giving a bistable magnet. In addition, light-induced excited spin-state trapping (LIESST)-like effects for copper−nitroxide complexes were reported very recently.[46] We are now searching for materials showing a LIESST-like effect from our compounds.

4. Experimental Section

Preparation of $\mathbf{1}\cdot BF_4$ ($[Cu(2pyNO^-)(2pyNO^\bullet)]_2(BF_4)_2$). A dichloromethane solution (0.5 mL) containing 34 mg (0.20 mmol) of 2pyNO[12b] and 34 mg (0.20 mmol) of 2pyNOH was combined to an ethanol solution (3 mL) containing 69 mg (0.20 mmol) of $Cu(BF_4)_2\cdot 6H_2O$. The yield of the black block crystals was 48 mg (0.050 mmol on the dinuclear basis; 25%). Mp 174−176 °C (dec). Anal. Calcd: C, 44.97; H, 5.45; N, 11.65 for $C_{36}H_{52}B_2Cu_2F_8N_8O_4$. Found: C, 44.76; H, 5.11; N, 11.30. IR (KBr disk) 521, 559, 779, 1063, 1084, 1124, 1196, 1437, 1468, 1608, 2939, 2983, 3097 cm^{-1}.

Preparation of $\mathbf{1}\cdot ClO_4$ ($[Cu(2pyNO^-)(2pyNO^\bullet)]_2(ClO_4)_2$). This compound was prepared according to practically the same way by using $Cu(ClO_4)_2\cdot 6H_2O$ in place of $Cu(BF_4)_2\cdot 6H_2O$. The yield was 37%. Mp 176−178 °C (dec). Anal. Calcd: C, 43.82; H, 5.31; N, 11.35 for $C_{36}H_{52}Cl_2Cu_2N_8O_{12}$. Found: C, 44.24; H, 5.07; N, 11.58. IR (KBr disk) 559, 623, 777, 1095, 1195, 1437, 1468, 1608, 2939, 2989, 3095 cm^{-1}.

X-ray Crystallographic Studies. X-ray diffraction data of a single crystal of $\mathbf{1}\cdot ClO_4$ were collected at 90 K on a Rigaku R-axis RAPID IP diffractometer with graphite monochromated Mo Kα ($\lambda = 0.71073$ Å) radiation. The structure was solved by direct methods and expanded using Fourier techniques in CRYSTALSTRUCTURE program package.[47] Numerical absorption correction was used. Full-matrix least-squares methods were applied using all of the unique reflection data. Thermal displacement parameters were refined anisotropically for non-hydrogen atoms. All of the hydrogen atoms were located at calculated positions, and the parameters were refined as "riding". Selected crystallographic data are summarized in Table 1.

As for $\mathbf{1}_{HT}\cdot BF_4$, X-ray diffraction data of a single crystal were collected at 300 K on a Rigaku Saturn70 CCD diffractometer with graphite monochromated Mo Kα ($\lambda = 0.71073$ Å) radiation. The low-temperature data of $\mathbf{1}_{LT}\cdot BF_4$ (50 K) were collected on the low-temperature vacuum camera installed at the BL02B1 beamline of the SPring-8 with Si(1 1 1) monochromated synchrotron radiation ($\lambda = 0.61792$ Å). The structure of each phase was solved by a direct method using the program SIR2004[48] and refined by a full-matrix least-squares method using the program SHELXL-97.[49] Empirical absorption corrections were applied. Other details are the same as those for $\mathbf{1}\cdot ClO_4$.

Magnetic Measurements. Magnetic susceptibilities of the polycrystalline samples were measured on a Quantum Design MPMS SQUID magnetometer at an applied magnetic field of 5000 Oe. The magnetic response was corrected with diamagnetic blank data of the sample holder obtained separately. The diamagnetic contribution of the sample itself was estimated from Pascal's constant.

EPR Measurements. EPR spectra were recorded on a JEOL JES-TE300 X-band (9.2 GHz) spectrometer equipped with a Heli-Tran model LTR-3 cryostat (APD Cryogenics) for low-temperature

(43) Becke, A. D. *J. Chem. Phys.* **1993**, *98*, 5648.
(44) Lee, C.; Yang, W.; Parr, R. G. *Phys. Rev. B* **1998**, *37*, 785.
(45) Frisch, M. J.; et al. *Gaussian03*, revisionC.02; Gaussian, Inc.: Wallingford CT, 2004.
(46) Fedin, M.; Ovcharenko, V.; Sagdeev, R.; Reijerse, E.; Lubotz, W.; Bagryanskaya, E. *Angew. Chem., Int. Ed.* **2008**, *47*, 6897.
(47) *CrystalStructure: Crystal Structure Analysis Package*, version3.8; Rigaku/MSC: The Woodlands, TX2000−2006.
(48) Burla, M. C.; Caliandro, R.; Camalli, M.; Carrozzini, B.; Cascarano, G. L.; De Caro, L.; Giacovazzo, C.; Polidori, G.; Spagna, R. *J. Appl. Crystallogr.* **2005**, *38*, 381.
(49) Sheldrich, G. M. *Acta Crystallogr., Sect. A* **2008**, *64*, 112.

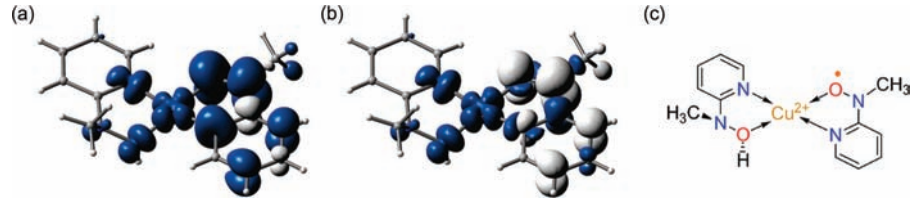

Figure 9. Spin density surfaces for (a) the ground triplet state and (b) the broken-symmetry singlet state of $\mathbf{1}_{HT}\cdot BF_4$. They were calculated on the UB3LYP/6-311G(d,p) level. Dark blue, positive spin; light gray, negative spin. (c) The structural formula for the model compound.

Table 3. Experimental Values for J and ϕ and Calculated Values for $E_{singlet}$, $E_{triplet}$, and J_{calc} on a Simplified Model Molecule

compounds	$2J\ k_B^{-1}$/K	$\lvert\phi\rvert$/deg	$E_{singlet}$/au	$E_{triplet}$/au	$2J_{calc}\ k_B^{-1}$/K
$\mathbf{1}_{HT}\cdot BF_4$	+74(16)	4.5(3)	−2475.65333243	−2475.65404570	+236
$\mathbf{1}_{LT}\cdot BF_4$	−778(12)	19.34(8)	−2475.69967142	−2475.69734370	−764
$\mathbf{1}\cdot ClO_4$	+218(4)	2.1(2)	−2475.69996845	−2475.70102947	+352

experiments. Saturation effects were carefully removed from the spectra by lowering the microwave power. The specimen in a quartz cell tube was evacuated by an oil rotary pump and then charged ~30 mmHg helium gas for heat exchange.

Powder X-ray Diffraction (XRD). Powder XRD patterns of $\mathbf{1}\cdot BF_4$ were collected on a MacScience MXP21TA diffractometer with Cu Kα (λ = 1.54184 Å) radiation. A graphite counter monochromator was applied. The range of each scan was 8−30° in 2θ measured by $2\theta/\theta$ scan; a counting time of each step was 3 s with an interval of 0.02°. Measuring temperatures were controlled by thermal conduction using a helium closed-cycle compressor system, RDK-205D, Sumitomo Heavy Industries, Ltd. Temperature was varied from 300 to 10 K, and then was raised to 300 K. During the variation of temperature, the data were collected at 300, 200, 100, from 80 to 30 K each 5 K, 20, and 10 K in cooling and heating processes. The variation rate was 2 K min^{-1}, and the specimen was kept for 30 min at a target temperature before each scan. Cell parameters were refined by the Pawley method.[50]

Specific Heat Measurements. Specific heat measurements were performed by the thermal relaxation method using a PPMS (Quantum Design) down to 1.9 K. Several pieces of block crystals (1.48 mg) were attached on the sample holder by a small amount of Apiezon N grease. The heat capacity of the sample holder including the grease is subtracted from the total heat capacity data.

Density Functional Theory Calculation. Molecular orbital calculations were performed with the Gaussian03 program.[45] We applied unrestricted DFT UB3LYP methods with the Becke exchange functional[43] and the Lee−Yang−Parr correlation functional.[44] The 6-311G(d,p) basis set was chosen. The convergence criterion for the energy was set at 10^{-9} au. The Hartree−Fock energies of the singlet states were obtained according to the broken symmetry method.[51] The singlet and triplet states of the monomer units in **1** were investigated in the calculation at the same level. The *tert*-butyl groups were replaced with methyl groups for reduction of calculation cost. The cut section of the monomer unit (oxygen atom of the $2pyNO^-$ moiety) was capped with a hydrogen atom. Single-point energy calculation was performed with the use of the geometrical parameters determined from X-ray crystallography except for the modification described above. We evaluated the coupling constant from the calculated energies of the high-spin (triplet) and broken-symmetry (singlet) states, according to eq 3.[51]

$$J = \frac{E_{BS} - E_{HS}}{\langle S^2\rangle_{HS} - \langle S^2\rangle_{BS}} \tag{3}$$

Acknowledgment. This work was partly supported by Grants-in-Aid for Scientific Research from the Ministry of Education, Culture, Sports, Science and Technology, Japan (Nos. 19550135 and 21110513). A.O. acknowledges JSPS for financial support (No. 20011509). Prof. Norimichi Kojima (The University of Tokyo) is acknowledged for valuable discussion. We express their thanks to Prof. Koshiro Toriumi, Prof. Yoshiki Ozawa, and Dr. Takayoshi Ito for kind assistance with synchrotron radiation experiments. The synchrotron radiation experiments were performed at the BL02B1 in the SPring-8 with the approval of the Japan Synchrotron Radiation Research Institute (JASRI) (Proposal No. 2007A1935).

Supporting Information Available: Figure S1 and S2, complete ref 45 and crystallographic information files (CIF) for $\mathbf{1}_{HT}\cdot BF_4$, $\mathbf{1}_{LT}\cdot BF_4$, and $\mathbf{1}\cdot ClO_4$. This material is available free of charge via the Internet at http://pubs.acs.org.

JA102163D

(50) Pawley, G. S. *J. Appl. Crystallogr.* **1981**, *14*, 357.

(51) (a) Ruiz, E.; Cano, J.; Alvarez, S.; Alemany, P. *J. Comput. Chem.* **1999**, *20*, 1391. (b) Nishino, M.; Yamanaka, S.; Yoshioka, Y.; Yamaguchi, K. J. *Chem. Phys. A* **1997**, *101*, 705. (c) Constantinides, C. P.; Koutentis, P. A.; Schatz, J. *J. Am. Chem. Soc.* **2004**, *126*, 16232.